Lewis number and preferential diffusion effects in lean hydrogen–air highly turbulent flames

Citation for the original published paper (version of record):
Lee, H., Dai, P., Wan, M. et al (2022). Lewis number and preferential diffusion effects in lean hydrogen–air highly turbulent flames. Physics of Fluids, 34(3). http://dx.doi.org/10.1063/5.0087426

(article starts on next page)

Physics of Fluids

RESEARCH ARTICLE | MARCH 21 2022

Lewis number and preferential diffusion effects in lean hydrogen–air highly turbulent flames

Special Collection: Development and Validation of Models for Turbulent Reacting Flows

Hsu Chew Lee (李树洲) ; Peng Dai (戴鹏) ; Minping Wan (万敏平) ; Andrei N. Lipatnikov

Physics of Fluids 34, 035131 (2022)
https://doi.org/10.1063/5.0087426

Physics of Fluids ARTICLE scitation.org/journal/phf

Lewis number and preferential diffusion effects in lean hydrogen–air highly turbulent flames

Cite as: Phys. Fluids **34**, 035131 (2022); doi: 10.1063/5.0087426
Submitted: 5 February 2022 · Accepted: 4 March 2022 ·
Published Online: 21 March 2022

Hsu Chew Lee (李树洲),[1,2,3] Peng Dai (戴鹏),[1] Minping Wan (万敏平),[1,2,3] and Andrei N. Lipatnikov[4,a)]

AFFILIATIONS

[1]Guangdong Provincial Key Laboratory of Turbulence Research and Applications, Department of Mechanics and Aerospace Engineering, Southern University of Science and Technology, Shenzhen, Guangdong 518055, China
[2]Guangdong-Hong Kong-Macao Joint Laboratory for Data-Driven Fluid Mechanics and Engineering Applications, Southern University of Science and Technology, Shenzhen 518055, China
[3]Southern Marine Science and Engineering Guangdong Laboratory (Guangzhou), Guangzhou 511458, People's Republic of China
[4]Department of Mechanics and Maritime Sciences, Chalmers University of Technology, Gothenburg SE-412 96, Sweden

Note: This paper is part of the special topic, Development and Validation of Models for Turbulent Reacting Flows.
[a)]**Author to whom correspondence should be addressed:** lipatn@chalmers.se

ABSTRACT

Unsteady three-dimensional direct numerical simulations of highly turbulent, complex-chemistry, lean hydrogen-air flames were performed by changing the equivalence ratio ϕ, root mean square velocity u', and turbulence length scale L. For each set of $\{\phi, u', L\}$, to explore the influence of molecular transport coefficients on the turbulent burning velocity U_T, four cases were designed: (i) mixture-averaged diffusivities; (ii) diffusivities equal to the heat diffusivity κ of the mixture for all species; (iii) mixture-averaged diffusivities for all species with the exception of O_2, whose diffusivity was equal to the diffusivity D_{H_2} of H_2 to suppress preferential diffusion effects; and (iv) mixture-averaged diffusivities multiplied with κ/D_{H_2} to suppress Lewis number effects but retain preferential diffusion effects. The computed results show a significant increase in U_T due to differences in molecular transport coefficients even at Karlovitz number Ka as large as 565. The increase is documented in cases (i) and (iii) but is not observed in case (iv)—indicating that this phenomenon is controlled by Lewis number effects, whereas preferential diffusion effects play a minor role. The phenomenon is more pronounced in leaner flames, with all other things being equal. While the temperature profiles $\langle T|c_F\rangle(c_F)$ conditionally averaged at the local value of the combustion progress variable c_F and sampled from the entire flame brushes are not sensitive to variations in molecular transport coefficients at high Ka, the $\langle T|c_F\rangle(c_F)$-profiles sampled from the leading edges of the same flame brushes show significant increase in the local temperature in cases (i) and (iii) characterized by a low Lewis number.

I. INTRODUCTION

Due to the threat of global warming, there has been a rapidly growing interest in the conversion of energy bond in renewable carbon-free fuels such as H_2. From the combustion perspective, to facilitate transition to carbon-free energetics and transport, there is an urgent need for developing models capable of predicting major characteristics of lean turbulent burning of H_2 or fuel blends that contain molecular hydrogen (CH_4/H_2, NH_3/H_2, or syngas). While significant progress has recently been made in understanding both the influence of turbulence on a premixed flame[1–6] and the influence of combustion-induced thermal expansion on turbulence,[7–12] a crucial unresolved challenge associated with lean turbulent burning of H_2 consists of predicting the abnormally high turbulent flame speeds well documented in experiments with lean H_2–air, syngas–air, and NH_3/H_2–air mixtures, see a review article[13] and more recent papers.[14–19]

This phenomenon is commonly attributed to local changes in the equivalence ratio and temperature due to the imbalance of (i) molecular fluxes of fuel and oxygen or (ii) molecular fluxes of reactants and heat to/from the reaction zones curved and strained by turbulent eddies.[13,20,21] The former and latter mechanisms are known as preferential diffusion and Lewis number effects, respectively. In the case of a laminar flow and single-step chemistry, activation energy asymptotic theories describe such effects in weakly stretched[22,23] and slowly varying[24,25] flames of an arbitrary configuration or in critically strained counter-flow[20,26] flames. Some of these theories[24,25] predict that Lewis number effects overwhelm preferential diffusion effects if the mixture

composition is far from stoichiometric. Other theories[20] imply the importance of preferential diffusion effects also. When discussing molecular transport effects in complex-chemistry turbulent flames, both Lewis number and preferential effects are often considered. Certain models of turbulent combustion highlight the latter effects,[20,27] whereas instantaneous two-dimensional images of hydrogen mass fraction, temperature, and fuel consumption rate, obtained by Aspden[28] from a single moderately turbulent flame invoking different models of molecular transport, indicate that the preferential diffusion effects are of minor importance when compared to the Lewis number effects. However, changes in turbulent burning velocity caused by these two effects have not yet been compared; this work aimed initially at filling this knowledge gap by analyzing results of a specially designed set of direct numerical simulations (DNSs). Since other results obtained by analyzing the DNS data appear to be of interest, some of them will also be presented in the following.

In Sec. II, the DNS attributes are briefly reported. Numerical results are discussed in Sec. III, followed by conclusions.

II. DNS ATTRIBUTES

Since the DNS attributes have already been discussed in detail elsewhere,[29–31] only a brief summary of the simulations is provided below. Statistically planar and one-dimensional, unconfined, lean H_2–air turbulent flames were simulated using a detailed chemical mechanism (nine species, 22 reactions) by Kéromnès *et al.*[32] Unsteady three-dimensional continuity, Navier–Stokes, and transport equations written in the low-Mach-number approximation were numerically integrated by adopting the solver *DINO*[33] in a rectangular computational domain of $\Lambda \times 16\Lambda \times \Lambda$. The domain was covered with a uniform Cartesian mesh of $N_x \times 16N_x \times N_x$ cells. Along the streamwise y-direction, the inflow and outflow boundary conditions were set. Other boundary conditions were periodic.

In a layer of $0.5\Lambda \le y \le 8\Lambda$, the linear forcing method[34,35] was applied to generate turbulence. The turbulence characteristics are reported elsewhere.[29] In a single case C, one more DNS was run by switching off turbulence generation, i.e., the turbulence decayed in time, with all other things being equal. As discussed elsewhere,[29,30] this change of turbulence evolution did not change the major effects of small-scale turbulence on the local burning.

The simulation conditions are reported in Table I, where ϕ is the equivalence ratio; S_L and $\delta_L^T = (T_b - T_u)/\max\left\{|dT/dy|\right\}$ are the laminar flame speed and thickness, respectively, pre-computed using the same chemical mechanism[32] and code *Cantera*[36] under room conditions; u' and L are the root mean square turbulent velocity and integral length scale, respectively; $Da = \tau_t/\tau_f$ is the Damköhler number; $Ka = (u'/S_L)^{3/2}\left(\delta_L^T/L\right)^{1/2}$ is the Karlovitz number; $Re_t = u'L/\nu_u$ is the turbulent Reynolds number; T designates the temperature; $\tau_t = L/u'$ and $\tau_f = \delta_L^T/S_L$ are the turbulence time scale and the laminar flame time scale, respectively; ν_u is the kinematic viscosity of unburned mixture; $\eta = LRe_t^{-3/4}$ is the Kolmogorov length scale; Δx is the mesh step; and the subscripts u and b designate unburned and burned mixtures, respectively. Reported in the two right-most columns are time-averaged values of dimensional and normalized burning velocity evaluated as follows:

$$U_t^F(t) = \frac{1}{(\rho Y_{H_2})_u \Lambda^2} \iiint_\Omega |\dot{\omega}_{H_2}|(\mathbf{x}, t) d\mathbf{x}. \tag{1}$$

Here, ρ is the density, Y_{H_2} is the fuel mass fraction, $\dot{\omega}_{H_2}$ is the fuel consumption rate, and Ω designates the computational domain.

DNS data obtained in cases C and C1 were analyzed in our earlier papers.[29–31] New cases D and D1, E and E1, and F and F1 were designed to explore the Lewis number and preferential diffusion effects under various equivalence ratios, u'/S_L, and L/δ_L^T. First, flames C and D propagate in the statistically same turbulence regime but are

TABLE I. Major characteristics of simulated flames.

Case	ϕ	S_L, m/s	δ_L^T, mm	$\frac{u'}{S_L}$	$\frac{L}{\delta_L^T}$	Da	Ka	Re_t	$\frac{\Delta x}{L}$	$\frac{\Delta x}{\eta}$	N_x	Λ, mm	$\overline{U_T^F(t)}$ m/s	$\frac{\overline{U_T^F(t)}}{S_L}$
C	0.5	0.58	0.41	11.2	1.10	0.10	33.0	158	0.041	1.85	128	2.4	5.14	8.86
C/O_2	0.5	0.59	0.42	11.1	1.10	0.10	35.5	158	0.041	1.85	128	2.4	5.17	8.82
C/T	0.5	0.80	0.30	8.2	1.50	0.19	18.8	158	0.041	1.85	128	2.4	2.55	3.20
C1	0.5	0.78	0.29	8.3	1.60	0.19	19.0	158	0.041	1.85	128	2.4	3.32	4.26
D	0.35	0.12	0.92	54.1	0.49	0.017	565	160	0.041	1.85	128	2.4	1.78	14.9
D/O_2	0.35	0.13	0.83	49.4	0.52	0.011	481	160	0.041	1.85	128	2.4	2.03	15.4
D/T	0.35	0.29	0.43	21.9	1.05	0.05	100	160	0.041	1.85	128	2.4	1.02	3.42
D1	0.35	0.30	0.43	21.6	1.10	0.05	97	160	0.041	1.85	128	2.4	1.08	3.61
E	0.35	0.12	0.92	11.2	0.50	0.04	53.2	33	0.082	1.13	64	2.4	1.49	12.4
E/O_2	0.35	0.13	0.83	10.2	0.52	0.05	45.2	33	0.082	1.13	64	2.4	1.72	13.1
E/T	0.35	0.29	0.43	4.5	1.02	0.23	9.4	33	0.082	1.13	64	2.4	0.48	1.6
E1	0.35	0.30	0.43	4.5	1.07	0.24	9.1	33	0.082	1.13	64	2.4	0.66	2.2
F	0.35	0.12	0.92	11.2	1.15	0.10	34.8	77	0.041	1.07	128	5.6	2.70	22.5
F/O_2	0.35	0.13	0.83	10.2	1.22	0.12	29.6	77	0.041	1.07	128	5.6	2.70	20.5
F/T	0.35	0.29	0.43	4.5	2.45	0.54	6.14	77	0.041	1.07	128	5.6	1.04	3.5
F1	0.35	0.30	0.43	4.5	2.50	0.56	5.96	77	0.041	1.07	128	5.6	1.37	4.5

characterized by different ϕ and, hence, by different S_L, δ_L^T, or τ_f. Accordingly, the values of u'/S_L, L/δ_L^T, Da, or Ka are also different for the two flames. Second, flames D and E are characterized by different u' (and, hence, different Da or Ka), but the same ϕ or L/δ_L^T. In addition, flames C and E are characterized by approximately equal ratios of u'/S_L, but different ϕ, L/δ_L^T, Da, or Ka. Third, in case F, the domain width Λ and the length scale L are increased for the values of u'/S_L, L/δ_L^T, Da, or Ka to be approximately equal in cases C and F. Thus, the major difference between these two cases consists of the equivalence ratio. Among the eight aforementioned cases, flame D is characterized by the lowest Da and the highest Ka.

The sole difference between cases $\mathcal{L}$ and $\mathcal{L}1$, where $\mathcal{L}$ subsumes a capital letter (C, D, E, or F), consists of changing the mixture-averaged molecular diffusivities $D_k \neq \kappa$ (cases $\mathcal{L}$) to $D_k = \kappa$ for all species k (cases $\mathcal{L}1$). Here, κ is the molecular heat diffusivity of the mixture. In cases $\mathcal{L}1$, the computed S_L is larger, in line with the theory of laminar premixed flames.[26] Cases $\mathcal{L}/O_2$ and $\mathcal{L}/T$ were designed to compare the magnitudes of the Lewis number and preferential diffusion effects. More specifically, to suppress the latter effects in cases $\mathcal{L}/O_2$, cases $\mathcal{L}$ were modified by setting $D_{O_2} = D_{H_2}$, with all other input parameters being unchanged. To suppress the former effects in case $\mathcal{L}/T$, cases $\mathcal{L}$ were modified by multiplying the molecular diffusivities of all species with κ/D_{H_2}. For the studied lean H_2–air mixtures, the Lewis number $Le = \kappa/D_{H_2} = 0.39$ in case C and 0.36 in cases D, E, F. Thus, the preferential diffusion mechanism is eliminated in flames $\mathcal{L}/O_2$, which are still subject to Lewis number effects, whereas the latter effects are eliminated in flames $\mathcal{L}/T$, which are still subject to preferential diffusion.

Each turbulent flame was initialized by embedding a pre-computed steady, planar, one-dimensional laminar flame solution at $y = 8N_x$. When necessary, the mean inlet velocity was manually changed to keep the flame within the forced-flow subdomain. Statistics was sampled after a transition stage, whose duration was equal to $3\tau_t$ (case F), $5\tau_t$ (other F-flames), $15\tau_t$ (cases C, C/T, and C1), or $10\tau_t$ (all other flames). When processing the DNS data, conventional or conditional averaging was applied across the transverse planes $y =$ const. For an arbitrary quantity q, its instantaneous transverse-averaged value is designated with $\langle q \rangle (y, t)$ in the following, whereas overbar refers to time averaging, performed over at least $25\tau_t$.

The combustion progress variable is defined using the fuel mass fraction, i.e., $c_F = (Y_{H_2,u} - Y_{H_2})/Y_{H_2,u}$, and the local equivalence ratio is equal to

$$\phi = \frac{1}{2}\frac{2X_{H_2} + 2X_{H_2O} + X_H + X_{OH} + X_{HO_2} + 2X_{H_2O_2}}{2X_{O_2} + X_{H_2O} + X_O + X_{OH} + 2X_{HO_2} + 2X_{H_2O_2}}, \quad (2)$$

where X_S is the mole fraction of species S.

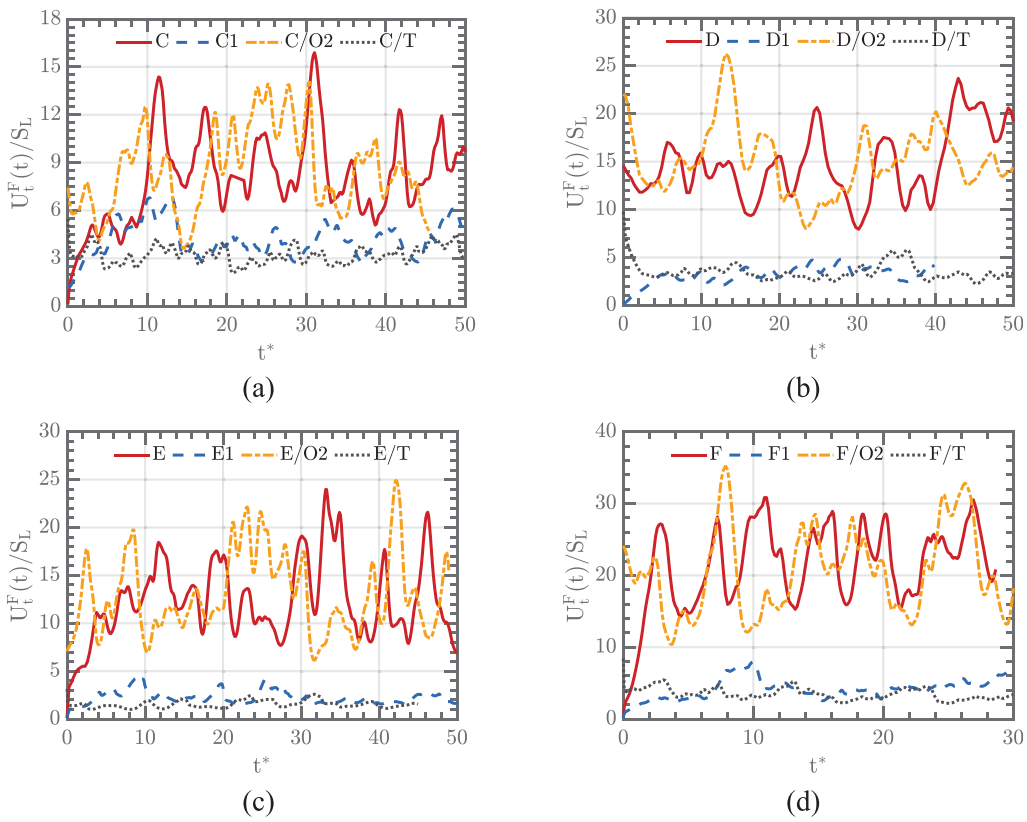

FIG. 1. Dependencies of the normalized turbulent burning velocities $U_T^F(t)/S_L$ on the normalized time $t^* = t/\tau_t$, computed in (a) C, (b) D, (c) E, and (d) F sets of flames. Case names are reported in legends.

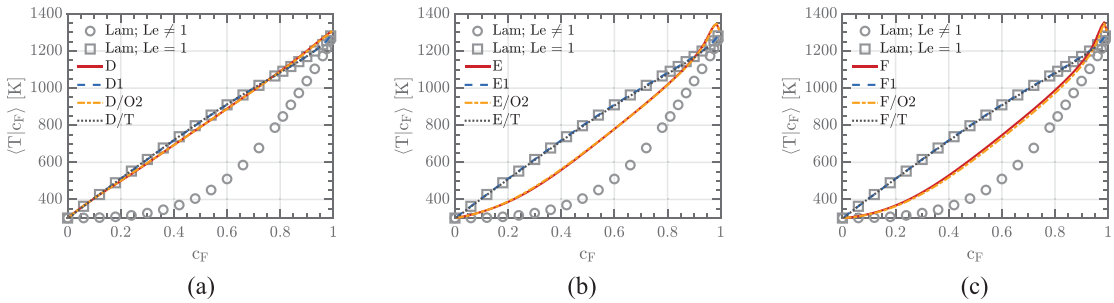

FIG. 2. Conditioned temperatures extracted from entire flame brushes in cases $\mathcal{L}$ (red solid lines), $\mathcal{L}/O_2$ (orange dotted-dashed lines), $\mathcal{L}$/T (black dotted lines), and $\mathcal{L}1$ (blue dashed lines). The circles and squares show $T(c_F)$ obtained from low Lewis number and equidiffusive unperturbed laminar flames, respectively, corresponding to cases D–F and D1–F1, respectively. (a) D, (b) E, and (c) F sets of flames.

III. RESULTS AND DISCUSSION

Figure 1 shows the dependencies of the normalized turbulent burning velocities $U_T^F(t)/S_L$ on the normalized time $t^* = t/\tau_t$, with the time-averaged burning velocities being reported in Table I. The following trends are worth emphasizing.

First, a comparison of the curves plotted in red solid and blue dashed lines shows that an increase in the turbulent burning rate due to differences in molecular transport coefficients is well pronounced in all sets of flames. For instance, the ratio $\mathbb{R} = \left(\overline{U_T^F}/S_L\right)_{\mathcal{L}} / \left(\overline{U_T^F}/S_L\right)_{\mathcal{L}1}$ of the normalized turbulent burning velocities computed in low Lewis number cases $\mathcal{L}$ and equidiffusive cases $\mathcal{L}1$ is equal to 2.1, 4.1, 5.7, and 5.0 for C, D, E, and F sets of flames, respectively. The effect is significant even at Ka as large as 565 (case D), while $\mathbb{R}$ decreases from 5.7 to 4.1 with an increase in u'/S_L from 11 (case E) to 54 (case D). At the same time, $\mathbb{R}$ is larger at $Ka = 53$ (case E) when compared to $Ka = 35$ (case F). Moreover, $\mathbb{R}$ is significantly larger in a leaner flame F than in flame C despite the major non-dimensional characteristics (u'/S_L, L/δ_L^T, Da, and Ka) of the two flames being almost equal. Even the dimensional values of $\overline{U_T^F}$ are significantly larger in cases $\mathcal{L}$ than in equidiffusive cases $\mathcal{L}1$ despite the opposite trend being observed for S_L.

Second, a comparison of the curves plotted in orange dotted-dashed lines and black dotted lines with the curves plotted in red solid lines shows that, in cases $\mathcal{L}/O_2$, U_T^F/S_L is close to large U_T^F/S_L in cases $\mathcal{L}$ and is significantly larger than U_T^F/S_L in cases $\mathcal{L}$/T. Moreover, in the latter cases, U_T^F/S_L is comparable with low U_T^F/S_L in cases $\mathcal{L}1$, cf. curves plotted in black dotted and blue dashed lines. The same trends hold for the time-averaged burning velocity, see Table I. Thus, in all four low Lewis number flames $\mathcal{L}$, a significant increase in U_T^F/S_L when compared to equidiffusive flames $\mathcal{L}1$ is controlled by the Lewis number effects. Preferential diffusion effects play a minor (if any) role.

On the contrary, Fig. 2(a) does not show an increase in conditioned temperatures $\langle T|c_F\rangle$ extracted from entire flame brushes in cases D and D/O_2 when compared to cases D1 and D/T. Moreover, all four conditioned profiles of $\langle T|c_F\rangle$, extracted from the turbulent flames, are very close to a profile of $T(c_F)$ obtained from the equidiffusive unperturbed laminar flame (squares), corresponding to cases D1–F1. These results computed at the highest Ka, see Table I, are in line with earlier DNS findings,[37–40] which indicated that an increase in Ka resulted in vanishing sensitivity of the conditioned profiles of species concentrations and temperature to differences in molecular transport coefficients. However, Fig. 2(a) appears to be inconsistent with Fig. 1(b) at first glance.

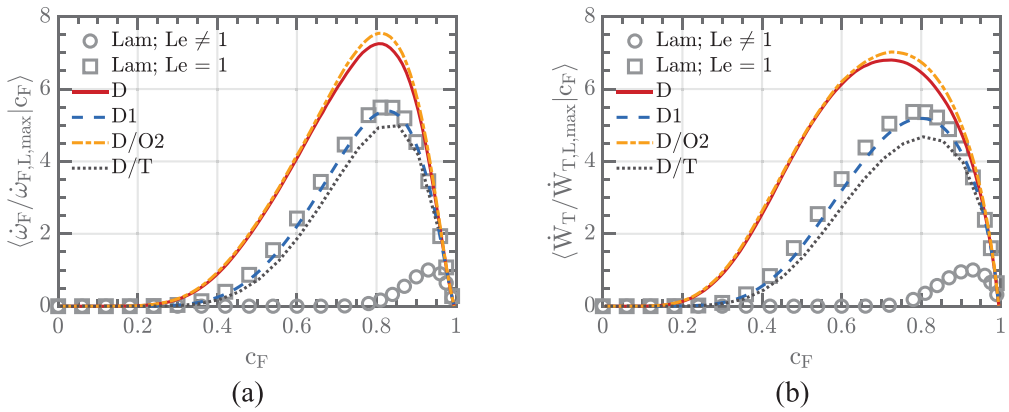

FIG. 3. Conditioned (a) fuel consumption and (b) heat release rates sampled from entire flame brushes and normalized using the highest rates in the low Le laminar flame. D-set of cases. Line legends are explained in caption to Fig. 2. The circles and squares show the profiles obtained from the laminar counterparts of flames D and D1, respectively.

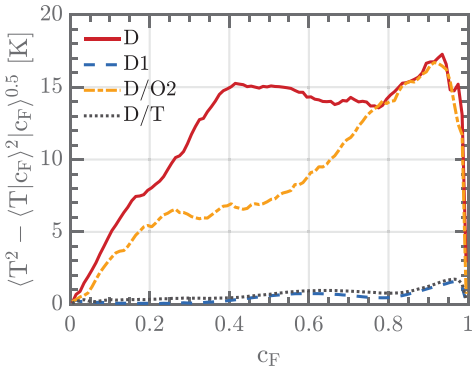

FIG. 4. Conditioned profiles of root mean square temperature $\left\langle T^2 - \langle T|c_F\rangle^2|c_F\right\rangle^{1/2}$ sampled from entire flame brushes in D-set of cases. Line legends are explained in caption to Fig. 2.

Furthermore, Figs. 2(b) and 2(c) show a decrease in $\langle T|c_F\rangle(c_F < 0.9)$ in flames E and E/O_2 or F and F/O_2 when compared to flames E1 and E/T or F1 and F/T, respectively, whereas Figs. 1(c) and 1(d) imply the opposite trend. The latter ($\mathcal{L}$/T and $\mathcal{L}$1) conditioned temperature profiles are again very close to $T(c_F)$ obtained from the equidiffusive unperturbed laminar flame (squares), whereas the former ($\mathcal{L}$ and $\mathcal{L}$/O_2) profiles lie between $T(c_F)$ obtained from the equidiffusive (squares) and low Lewis number (circles) laminar flames. Since flames E and F are characterized by Ka lower than in case D, these results further illustrate (in line with earlier studies[37–40]) that a sufficiently high Ka should be reached to suppress the sensitivity of conditioned profiles of temperature to differences in molecular transport coefficients.

The apparent inconsistency between the results plotted in Figs. 1 and 2 might be attributed to two effects. First, Fig. 3 shows that the conditioned fuel consumption and heat release rates sampled from the entire flame brushes are substantially higher in cases D and D/O_2 than in cases D1 and D/T despite approximately the same profiles $\langle T|c_F\rangle(c_F)$ reported in Fig. 2(a). This difference in the rates might be attributed to their highly non-linear dependencies on T and to different magnitudes of fluctuations of the local temperature in the studied flames. Figure 4 does show differences in the root mean square conditioned temperatures $\left\langle T^2 - \langle T|c_F\rangle^2|c_F\right\rangle^{1/2}$, but the magnitude of these differences appears to be too low to explain the rate differences in Fig. 3.

Second, it is worth stressing that the results reported in Figs. 2–4 have been sampled from entire flame brushes, whereas the

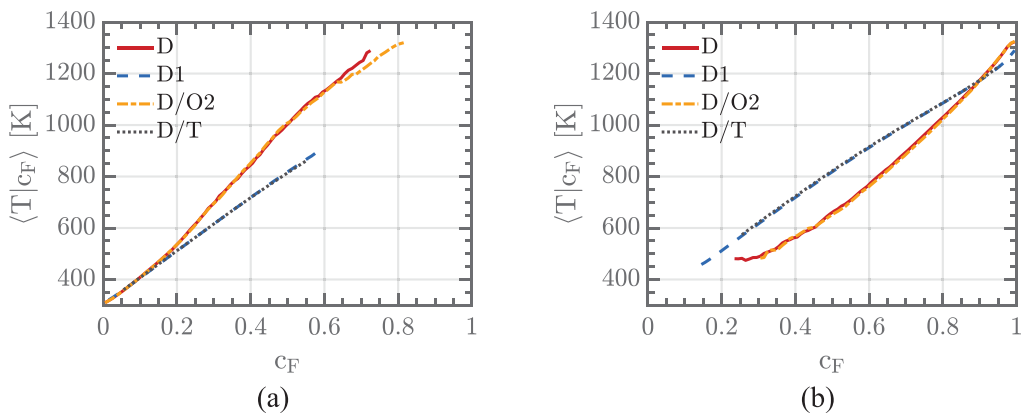

FIG. 5. Conditioned temperatures extracted from the (a) leading and (b) trailing edges of flame brushes. Line legends are explained in caption to Fig. 2. D-set of flames.

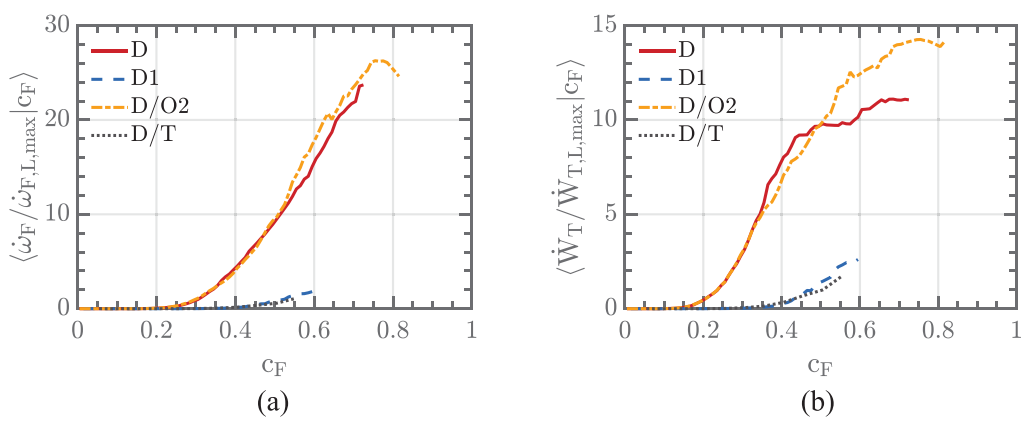

FIG. 6. Normalized conditioned (a) fuel consumption and (b) heat release rates sampled from the leading edges of flame brushes. Line legends are explained in caption to Fig. 2. D-set of flames.

conditioned profiles sampled from the leading or trailing edges of these flame brushes show very different behavior. For instance, Figs. 5(a) and 5(b) report the conditioned profiles $\langle T|c_F\rangle(c_F)$ sampled from layers characterized by $\langle c_F\rangle(y,t) = 0.1 \pm 0.005$ (leading edge) and $\langle c_F\rangle(y,t) = 0.9 \pm 0.005$ (trailing edge), respectively. Moreover, Figs. 6(a) and 6(b) show the conditioned fuel consumption and heat release rates, respectively, sampled from the leading edge. All these quantities sampled from the leading edges in cases D and D/O_2 are significantly larger than the counterpart quantities sampled from the leading edges in cases D/T and D1 (basically similar results obtained from C, E, and F sets of flames, characterized by a lower *Ka* are not shown for brevity).

The huge difference between conditioned fuel consumption or heat release rates, reported in Fig. 6, can make the conditioned rates different after averaging over the entire flame brush. Such an interpretation is supported by the fact that the conditioned rates are higher in case D/O_2 than in case D in both Figs. 3 and 6, whereas $\langle T^2 - \langle T|c_F\rangle^2|c_F\rangle^{1/2}$ shows the opposite behavior in Fig. 4.

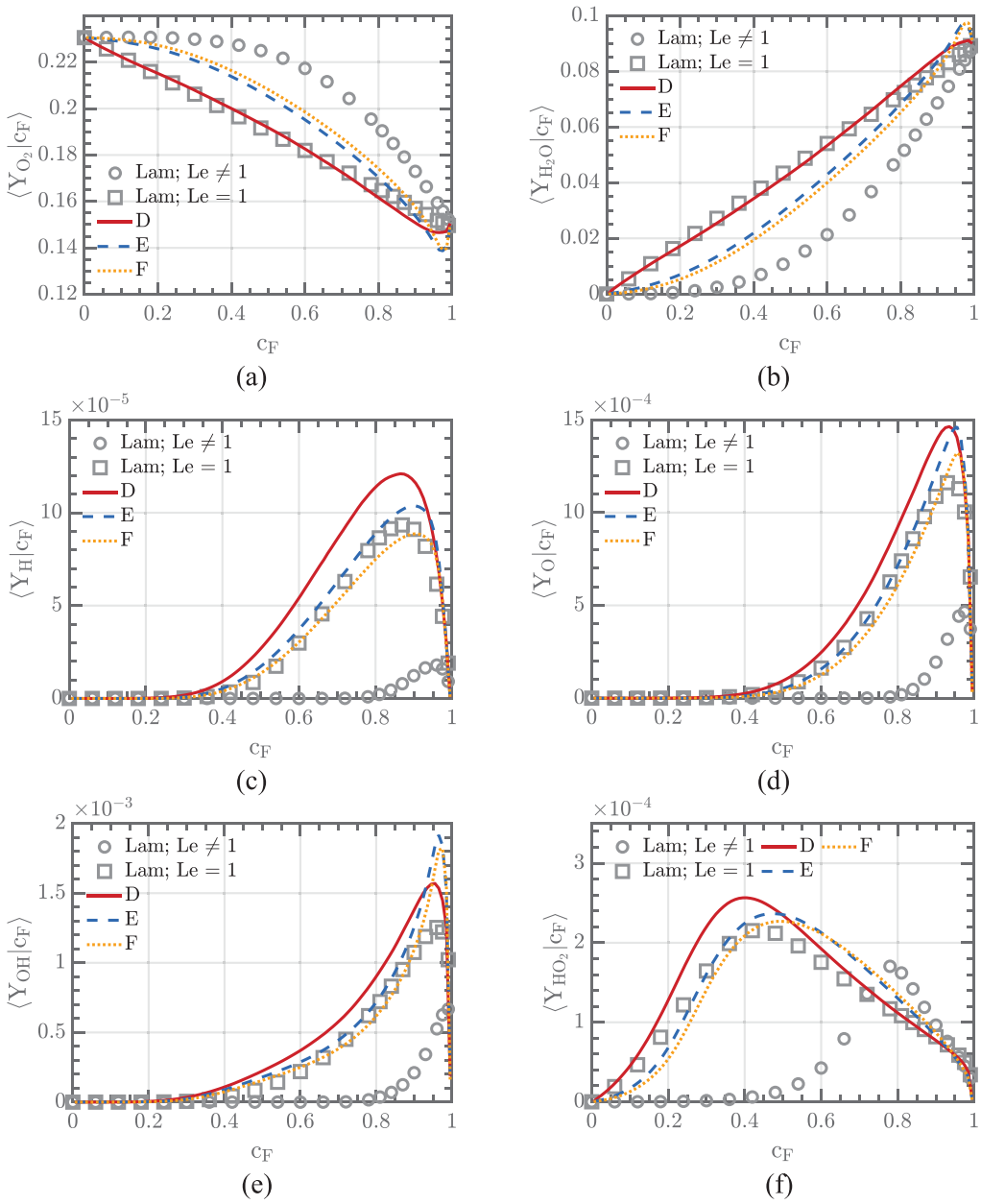

FIG. 7. Conditioned profiles of mass fractions of (a) O_2, (b) H_2O, (c) H, (d) O, (e) OH, and (f) HO_2, extracted from entire flame brushes in cases D (red solid lines), E (blue dashed lines), and F (orange dotted lines). Circles and squares show $Y_k(c_F)$ obtained from low Lewis number and equidiffusive laminar flames, respectively.

The highlighted differences, documented at the flame leading edges, are mainly associated with the dominance of highly and positively (products in curvature center) curved reaction zones near flame leading edge, as discussed in detail for flame C elsewhere.[31] Briefly speaking, if *Le* is significantly less than unity, temperature is locally increased in highly and positively curved reaction zones, because the molecular flux of chemical energy (bond in a light fuel with a high diffusivity) into these reaction zones overwhelms the heat flux from these zones. Such effects are well explored for stretched laminar flames.[20,22–26]

All the results reported in Figs. 1–6 are consistent with each other if the turbulent burning velocity is controlled by processes localized to the flame leading edge, in line with the leading point concept. As reviewed elsewhere,[13,20,26] the concept was pioneered by the Russian school. Subsequently, it was adapted to predict abnormally high turbulent burning velocities measured in very lean hydrogen flames.[41,42] Over the past decade, the concept was supported by analyzing experimental[14,16,17] or DNS[43–45] data, including data obtained from the present flames C and C1,[31] as well as in theoretical studies[46–48] and in Reynolds-averaged Navier–Stokes simulations[49] of Atlanta experiments[14,16] with lean syngas–air turbulent flames. Not only are the present DNS data consistent with the leading point concept, but they also strongly support it.

Thus, on the one hand, Figs. 1, 5, and 6 show that Lewis number effects should be taken into account when modeling turbulent burning velocity. On the other hand, Fig. 2 implies that such effects could be neglected when evaluating the conditioned temperature at high *Ka*. Such a simplification is also supported in Fig. 7, which shows that the conditioned profiles of species mass fractions either (i) tend to profiles obtained from the equidiffusive laminar flame (O_2 and H_2O) when *Ka* is increased or (ii) are sufficiently close to the equidiffusive laminar flame profiles (H, O, OH, and HO_2) at various *Ka*. This observation suggests that, even in lean H_2–air flames with pronounced Lewis number effects, the mean concentrations of various species in intense turbulence could be modeled by averaging a linear combination of the concentration profiles pre-computed for counterpart low Lewis number and equidiffusive laminar flames. The profile weights in such a linear combination could depend on *Ka* or/and another nondimensional flame characteristic (e.g., u'/S_L, L/δ_L^T, or *Da*). A comparison of Figs. 7(a) and 7(b) with Figs. 7(c)–7(f) implies that these weights could be different for major reactants or products and for radicals. This issue deserves further study and will be addressed in future publications.

IV. CONCLUSIONS

A significant increase in turbulent burning velocity U_T^F (both dimensional and normalized with the laminar flame speed S_L) due to differences in molecular transport coefficients is documented at a Karlovitz number *Ka* as high as 565.

The phenomenon is controlled by the Lewis number effects, whereas preferential diffusion plays a minor (if any) role.

This increase in U_T^F is more pronounced in leaner flames, with all other things being equal.

While the conditioned temperature profiles sampled from the entire flame brushes at high *Ka* are not sensitive to variations in molecular transport coefficients, similar profiles sampled from the leading edges of the flame brushes show significant increase in the local temperature in the case of a low Lewis number. Such effects are even more pronounced for fuel consumption and heat release rates. These results are fully consistent with the computed increase in U_T^F due to Lewis number effects and further illuminate the crucial role played by processes localized to the leading edge of a turbulent flame brush in its propagation. Therefore, Lewis number effects should not be disregarded when evaluating the turbulent burning velocity even at high *Ka*.

On the contrary, the use of temperature and species mass fraction profiles pre-computed for equidiffusive laminar flames could work reasonably well when evaluating the mean temperature and species mass fractions provided that an advanced predictive model of the probability density function $P(c_F)$ is available. Readers interested in recent progresses in modeling $P(c_F)$ in premixed turbulent flames are referred to the latest publications.[50–57]

ACKNOWLEDGMENTS

This work has been supported in part by NSFC (Grant Nos. 91752201, 51976088, and 92041001), the Shenzhen Science and Technology Program (Grant Nos. KQTD20180411143441009 and JCYJ20210324104802005), the Department of Science and Technology of Guangdong Province (Grant Nos. 2019B21203001 and 2020B1212030001), Key Special Project for Introduced Talents Team of Southern Marine Science and Engineering Guangdong Laboratory (Guangzhou) (No. GML2019ZD0103), and by Project No. LCH-2019011 under the Joint Program of Shenzhen Clean Energy Research Institute and SUSTech through contract CERI-KY-2019–003. AL acknowledges the support provided by the Combustion Engine Research Center (CERC).

AUTHOR DECLARATIONS

Conflict of Interest

The authors have no conflicts to disclose.

DATA AVAILABILITY

The data that support the findings of this study are available from the corresponding author upon reasonable request.

REFERENCES

[1] Z. Wang and J. Abraham, "Effects of Karlovitz number on turbulent kinetic energy transport in turbulent lean premixed methane/air flames," Phys. Fluids **29**, 085102 (2017).
[2] R. Yu and A. N. Lipatnikov, "DNS study of dependence of bulk consumption velocity in a constant-density reacting flow on turbulence and mixture characteristics," Phys. Fluids **29**, 065116 (2017).
[3] L. Cifuentes, C. Dopazo, A. Sandeep, N. Chakraborty, and A. Kempf, "Analysis of flame curvature evolution in a turbulent premixed bluff body burner," Phys. Fluids **30**, 095101 (2018).
[4] V. A. Sabelnikov, R. Yu, and A. N. Lipatnikov, "Thin reaction zones in constant-density turbulent flows at low Damköhler numbers: Theory and simulations," Phys. Fluids **31**, 055104 (2019).
[5] A. Y. Klimenko, "The convergence of combustion models and compliance with the Kolmogorov scaling of turbulence," Phys. Fluids **33**, 025112 (2021).
[6] V. A. Sabelnikov and A. N. Lipatnikov, "Scaling of reaction progress variable variance in highly turbulent reaction waves," Phys. Fluids **33**, 085103 (2021).

[7]C. Dopazo, L. Cifuentes, and N. Chakraborty, "Vorticity budgets in premixed combusting turbulent flows at different Lewis numbers," Phys. Fluids **29**, 045106 (2017).
[8]A. N. Lipatnikov, V. A. Sabelnikov, S. Nishiki, and T. Hasegawa, "Combustion-induced local shear layers within premixed flamelets in weakly turbulent flows," Phys. Fluids **30**, 085101 (2018).
[9]A. N. Lipatnikov, V. A. Sabelnikov, S. Nishiki, and T. Hasegawa, "Does flame-generated vorticity increase turbulent burning velocity?," Phys. Fluids **30**, 081702 (2018).
[10]P. Brearley, U. Ahmed, N. Chakraborty, and A. N. Lipatnikov, "Statistical behaviours of conditioned two-point second-order structure functions in turbulent premixed flames in different combustion regimes," Phys. Fluids **31**, 115109 (2019).
[11]V. A. Sabelnikov, A. N. Lipatnikov, S. Nishiki, H. L. Dave, F. E. Hernández-Pérez, W. Song, and H. G. Im, "Dissipation and dilatation rates in premixed turbulent flames," Phys. Fluids **33**, 035112 (2021).
[12]N. Chakraborty, C. Kasten, U. Ahmed, and M. Klein, "Evolutions of strain rate and dissipation rate of kinetic energy in turbulent premixed flames," Phys. Fluids **33**, 125132 (2021).
[13]A. N. Lipatnikov and J. Chomiak, "Molecular transport effects on turbulent flame propagation and structure," Prog. Energy Combust. Sci. **31**(1), 1 (2005).
[14]P. Venkateswaran, A. Marshall, D. H. Shin, D. Noble, J. Seitzman, and T. Lieuwen, "Measurements and analysis of turbulent consumption speeds of H_2/CO mixtures," Combust. Flame **158**, 1602 (2011).
[15]S. Daniele, P. Jansohn, J. Mantzaras, and K. Boulouchos, "Turbulent flame speed for syngas at gas turbine relevant conditions," Proc. Combust. Inst. **33**, 2937 (2011).
[16]P. Venkateswaran, A. Marshall, J. Seitzman, and T. Lieuwen, "Scaling turbulent flame speeds of negative Markstein length fuel blends using leading points concepts," Combust. Flame **162**, 375 (2015).
[17]W. Zhang, J. Wang, Q. Yu, W. Jin, M. Zhang, and Z. Huang, "Investigation of the fuel effects on burning velocity and flame structure of turbulent premixed flames based on leading points concept," Combust. Sci. Technol. **190**, 1354 (2018).
[18]S. Yang, A. Saha, W. Liang, F. Wu, and C. K. Law, "Extreme role of preferential diffusion in turbulent flame propagation," Combust. Flame **188**, 498 (2018).
[19]C. Lhuillier, P. Brequigny, F. Contino, and C. Mounaïm-Rousselle, "Experimental investigation on ammonia combustion behavior in a spark-ignition engine by means of laminar and turbulent expanding flames," Proc. Combust. Inst. **38**, 5859 (2021).
[20]V. R. Kuznetsov and V. A. Sabelnikov, *Turbulence and Combustion* (Hemisphere Publishing Corporation, New York, 1990).
[21]D. Bradley, A. K. C. Lau, M. Lawes, and F. T. Smith, "Flame stretch rate as a determinant of turbulent burning velocity," Philos. Trans. R. Soc., A **338**, 359 (1992).
[22]P. Clavin, "Dynamical behavior of premixed flame fronts in laminar and turbulent flows," Prog. Energy Combust. Sci **11**(1), 1 (1985).
[23]M. Matalon, "Flame dynamics," Proc. Combust. Inst. **32**, 57 (2009).
[24]J. K. Bechtold and M. Matalon, "Effects of stoichiometry on stretched premixed flames," Combust. Flame **119**, 217 (1999).
[25]A. P. Kelley, J. K. Bechtold, and C. K. Law, "Premixed flame propagation in a confining vessel with weak pressure rise," J. Fluid Mech. **691**, 26 (2012).
[26]Y. B. Zeldovich, G. I. Barenblatt, V. B. Librovich, and G. M. Makhviladze, *The Mathematical Theory of Combustion and Explosions* (Consultants Bureau, New York, 1985).
[27]M. Nakahara and H. Kido, "A study of the premixed turbulent combustion mechanism taking the preferential diffusion effect into consideration," Mem. Fac. Eng. Kyushu Univ. **58**, 55 (1998).
[28]A. J. Aspden, "A numerical study of diffusive effects in turbulent lean premixed hydrogen flames," Proc. Combust. Inst. **36**, 1997 (2017).
[29]H. C. Lee, P. Dai, M. Wan, and A. N. Lipatnikov, "A DNS study of extreme and leading points in lean hydrogen–air turbulent flames—Part I: Local thermo-chemical structure and reaction rates," Combust. Flame **235**, 111716 (2022).
[30]H. C. Lee, P. Dai, M. Wan, and A. N. Lipatnikov, "A DNS study of extreme and leading points in lean hydrogen–air turbulent flames—Part II: Local velocity field and flame topology," Combust. Flame **235**, 111712 (2022).
[31]H. C. Lee, P. Dai, M. Wan, and A. N. Lipatnikov, "Influence of molecular transport on burning rate and conditioned species concentrations in highly turbulent premixed flames," J. Fluid Mech. **928**, A5 (2021).
[32]A. Kéromnès, W. K. Metcalfe, K. A. Heufer, N. Donohoe, A. K. Das, C.-J. Sung, J. Herzler, C. Naumann, P. Griebel, O. Mathieu, M. C. Krejci, E. L. Petersen, W. J. Pitz, and H. J. Curran, "An experimental and detailed chemical kinetic modeling study of hydrogen and syngas mixture oxidation at elevated pressures," Combust. Flame **160**, 995 (2013).
[33]A. Abdelsamie, G. Fru, T. Oster, F. Dietzsch, G. Janiga, and D. Thévenin, "Towards direct numerical simulations of low-Mach number turbulent reacting and two-phase flows using immersed boundaries," Comput. Fluids **131**, 123 (2016).
[34]B. Bobbitt, S. Lapointe, and G. Blanquart, "Vorticity transformation in high Karlovitz number premixed flames," Phys. Fluids **28**, 015101 (2016).
[35]B. Bobbitt and G. Blanquart, "Vorticity isotropy in high Karlovitz number premixed flames," Phys. Fluids **28**, 105101 (2016).
[36]D. Goodwin, N. Malaya, H. Moffat, and R. Speth, *Cantera: An Object-Oriented Software Toolkit for Chemical Kinetics, Thermodynamics, and Transport Processes* (Caltech, Pasadena, CA, 2009).
[37]A. J. Aspden, M. S. Day, and J. B. Bell, "Turbulence-flame interactions in lean premixed hydrogen: Transition to the distributed burning regime," J. Fluid Mech. **680**, 287 (2011).
[38]B. Savard and G. Blanquart, "An a priori model for the effective species Lewis numbers in premixed turbulent flames," Combust. Flame **161**, 1547 (2014).
[39]S. Lapointe, B. Savard, and G. Blanquart, "Differential diffusion effects, distributed burning, and local extinction in high Karlovitz premixed flames," Combust. Flame **162**, 3341 (2015).
[40]A. J. Aspden, M. S. Day, and J. B. Bell, "Towards the distributed burning regime in turbulent premixed flames," J. Fluid Mech. **871**, 1 (2019).
[41]V. Karpov, A. Lipatnikov, and V. Zimont, "A test of an engineering model of premixed turbulent combustion," Proc. Combust. Inst. **26**, 249 (1996).
[42]V. P. Karpov, A. N. Lipatnikov, and V. L. Zimont, "Flame curvature as a determinant of preferential diffusion effects in premixed turbulent combustion," in *Advances in Combustion Science: In Honor of Ya. B. Zel'dovich*, edited by W. A. Sirignano, A. G. Merzhanov, and L. De Luca (AIAA, Reston, VA, 1997), pp. 235–250.
[43]S. H. Kim, "Leading points and heat release effects in turbulent premixed flames," Proc. Combust. Inst. **36**, 2017 (2017).
[44]H. L. Dave, A. Mohan, and S. Chaudhuri, "Genesis and evolution of premixed flames in turbulence," Combust. Flame **196**, 386 (2018).
[45]A. N. Lipatnikov, N. Chakraborty, and V. A. Sabelnikov, "Transport equations for reaction rate in laminar and turbulent premixed flames characterized by non-unity Lewis number," Int. J. Hydrogen Energy **43**, 21060 (2018).
[46]V. A. Sabelnikov and A. N. Lipatnikov, "Transition from pulled to pushed premixed turbulent flames due to countergradient transport," Combust. Theory Model. **17**, 1154 (2013).
[47]V. A. Sabelnikov and A. N. Lipatnikov, "Transition from pulled to pushed fronts in premixed turbulent combustion: Theoretical and numerical study," Combust. Flame **162**, 2893 (2015).
[48]K. Q. N. Kha, V. Robin, A. Mura, and M. Champion, "Implications of laminar flame finite thickness on the structure of turbulent premixed flames," J. Fluid Mech. **787**, 116 (2016).
[49]S. Verma, F. Monnier, and A. N. Lipatnikov, "Validation of leading point concept in RANS simulations of highly turbulent lean syngas–air flames with well-pronounced diffusional-thermal effects," Int. J. Hydrogen Energy **46**, 9222 (2021).
[50]M. Pfitzner, "A new analytic pdf for simulations of premixed turbulent combustion," Flow. Turbul. Combust. **106**, 1213 (2021).
[51]M. Pfitzner and M. Klein, "A near-exact analytic solution of progress variable and pdf for single-step Arrhenius chemistry," Combust. Flame **226**, 380 (2021).
[52]M. Pfitzner and P. Breda, "An analytic probability density function for partially premixed flames with detailed chemistry," Phys. Fluids **33**, 035117 (2021).
[53]A. N. Lipatnikov and V. A. Sabelnikov, "Evaluation of mean species mass fractions in premixed turbulent flames: A DNS study," Proc. Combust. Inst. **38**, 6413 (2021).
[54]A. N. Lipatnikov and V. A. Sabelnikov, "An extended flamelet-based presumed probability density function for predicting mean concentrations of various species in premixed turbulent flames," Int. J. Hydrogen Energy **45**, 31162 (2020).

[55]A. N. Lipatnikov, V. A. Sabelnikov, F. E. Hernández-Pérez, W. Song, and, H. G. Im, "A priori DNS study of applicability of flamelet concept to predicting mean concentrations of species in turbulent premixed flames at various Karlovitz numbers," Combust. Flame **222**, 370 (2020).
[56]A. N. Lipatnikov, V. A. Sabelnikov, F. E. Hernández-Pérez, W. Song, and H. G. Im, "Prediction of mean radical concentrations in lean hydrogen–air turbulent flames at different Karlovitz numbers adopting a newly extended flamelet-based presumed PDF," Combust. Flame **226**, 248 (2021).
[57]A. N. Lipatnikov, T. Nilsson, R. Yu, X.-S. Bai, and V. A. Sabelnikov, "Assessment of a flamelet approach to evaluating mean species mass fractions in moderately and highly turbulent premixed flames," Phys. Fluids **33**, 045121 (2021).